A Thermoelectrical Approach for the Modelling of Different Ledge Regions in Aluminum Reduction Cells

André Felipe Schneider[1], Daniel Richard[2], Asbjørn Solheim[3] and Marc Dupuis[4]
1. Numerical Analysis Specialist – Center of Excellence for Aluminum, Hatch Ltd., Montréal, Canada
2.Associate – Center of Excellence for Aluminum, Hatch Ltd., Saguenay, Canada
3. Chief Scientist – SINTEF, Trondheim, Norway
4. Consultant, GeniSIM, Inc., Saguenay, Canada
Corresponding author: andre.schneider@hatch.com

Abstract

The energy balance of an aluminum reduction cell largely determines its operational window. A critical design concept is to dissipate enough heat to maintain a frozen layer of electrolyte (the ledge) that will protect the lateral surfaces of the lining from the aggressive bath. Experimental evidence shows that the upper ledge (facing bath) and the lower ledge (facing metal) have different chemical compositions. While the alumina content of the upper ledge is normally lower than in the bulk of the bath, the lower ledge is formed from an Al_2O_3-saturated solution close to the eutectic point. It is rationalized that this is the result of different mechanisms: the top portion is formed by direct freezing of the bulk bath, but the lower ledge originates from an entrained thin film of bath. However, most published energy balance models assume that the heat flux on the entire ledge surface is driven by a single superheat (*i.e.*, the difference between the bulk bath temperature and the liquidus temperature evaluated at the bulk bath composition). This paper proposes a methodology to converge the ledge profile using different melting temperatures for the distinct cavity regions, including a simplified representation of the ledge trench found at the bath-metal interface. This was implemented in the modernized ANSYS-based thermoelectrical model presented earlier [1]. The implications of this paradigm shift in the thermal design of an aluminum reduction cell are discussed by means of the numerical results obtained for a fictitious 300 kA cell technology.

Keywords: Aluminum reduction cells, Heat balance, Ledge trench, Liquidus temperature, Eutectic point.

1. Introduction

The energy balance of an aluminum reduction cell largely determines its operational window. A critical design concept is to dissipate enough heat to maintain a frozen layer of electrolyte (the ledge) that will protect the lateral surfaces of the lining from the aggressive bath. The prediction of the ledge profile can be quite challenging and numerical modeling is broadly employed to study the thermal-electrical behavior of the lining. The authors introduced in 2020 a modernized ANSYS-based thermoelectrical (TE) model [1] that builds upon the foundations first introduced and further developed by Dupuis [2–4] from the mid-1980s up to his most recent publications in the 2020s.

Dupuis' original approach relies on the iterative repositioning of the ledge front in a TE Finite Element (FE) model. The algorithm involves successive repositioning of the solidification front nodes based on the calculated temperature field until the entire ledge-to-liquids interface reaches the bath solidification temperature, T_{liq}. The superheat (*i.e.*, the difference between the bulk bath temperature and the liquidus temperature evaluated at the bulk bath composition, $\Delta T_{upper} = T_{opr} - T_{liq}$), is also adjusted while converging the ledge profile to minimize the difference between the cell internal heat generation and the integrated heat losses over the control volume.

This widely accepted methodology (and variants) assumes that the heat flux on the entire ledge surface is driven by a single superheat.

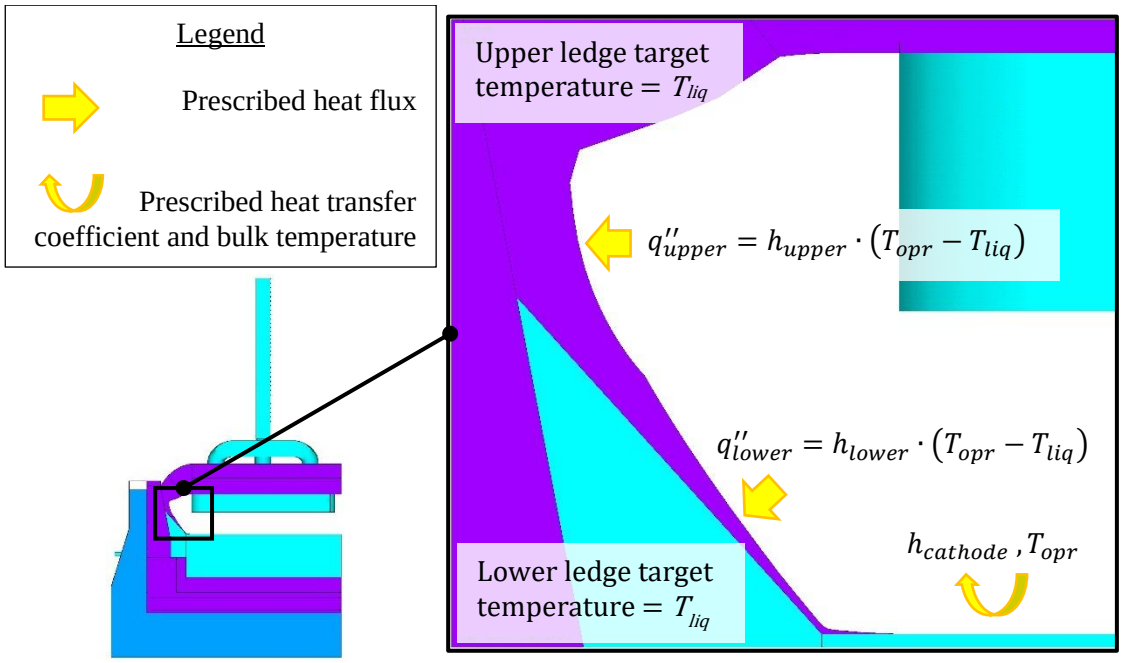

Figure 1. Upper ledge, lower ledge, and cathode panel thermal loads for a traditional FE-based energy balance model.

where:

q''_{upper} Prescribed heat flux at the upper ledge (facing bath), W/m^2
h_{upper} Uniform heat transfer coefficient at the upper ledge (facing bath), W/m^2·°C
T_{opr} Bulk bath temperature, °C
T_{liq} Liquidus temperature evaluated at the bulk bath composition, °C
q''_{lower} Prescribed heat flux at the lower ledge (facing metal), W/m^2
h_{lower} Uniform heat transfer coefficient at the lower ledge (facing metal), W/m^2·°C
$h_{cathode}$ Prescribed uniform heat transfer coefficient at the cathode panel surface, W/m^2·°C.

It is worth noting that this computational strategy is the basis for several successful aluminum reduction technologies designed by different parties, therefore unquestionably valuable from a design standpoint. Nevertheless, experimental evidence suggests that it cannot capture all the features of an industrial cell's ledge profile, as depicted in Figure 2. While models based on this strategy are able to capture the position of the ledge toe fairly well, the lower ledge (facing metal) tends to be either thicker or thinner than the computed profile. Most apparent is a remarkable reduction in the ledge thickness observed at the metal pad-bath interface. Finally, the upper portion (facing bath) of the measured ledge profile tends to be thicker than model predictions.

6. Conclusions

A methodology to converge the ledge profile using different melting temperatures for the distinct cavity regions, including a simplified representation of the ledge trench found at the bath-metal interface was implemented by leveraging the data structure of the modernized ANSYS-based TE FE model previously introduced by the authors. This methodology uses two distinct superheat definitions, namely, the traditional $\Delta T_{upper} = T_{opr} - T_{liq}$ at the bath level, and $\Delta T_{lower} = T_{alu} - T_{eut}$ at the metal pad level. The lower ledge superheat requires a reasonable estimation of both the bulk metal pad temperature and the bath film chemical composition. Finally, the simplified representation of the ledge trench is based on a parabolic heat transfer coefficient distribution that varies with the trench height.

Based on the obtained numerical results, it is the opinion of the authors that computation of a more realistic ledge profile requires considering both the unavoidable trench at the bath-metal interface and the different ledge formation mechanisms at metal pad and bath level. While the preliminary results are encouraging, validation against actual pots is required to determine both its reliability and usefulness as a design tool.

7. References

1. Daniel Richard et al., A modernized ANSYS-based finite element model for the thermal-electrical design of aluminum reduction cells, *Proceedings of the 38th International ICSOBA Conference*, Virtual Event, 16 to 18 November, 2020, Paper AL03, *Travaux* 49, 563-580.
2. Marc Dupuis & Imad Tabsh, Thermo-electric coupled field analysis of aluminium reduction cells using the ANSYS parametric design language, *Proceedings of the ANSYS Fifth International Conference*, Vol 3, 1991, 1780-1792.
3. Marc Dupuis, Thermo-electric design of a 400 kA cell using mathematical models: a tutorial, *Light Metals* 2000, 297-302.
4. Marc Dupuis, Computation of aluminium reduction cell energy balance using ANSYS® finite element models, *Light Metals* 1998, 409-417.
5. Marc Dupuis, Computation of accurate horizontal current density in metal pad using a full quarter cell thermo-electric model, *Proceedings of CIM* 2001, 3-11.
6. Marc Dupuis, How to limit the heat loss of anode stubs and cathode collector bars in order to reduce cell energy consumption, *Light Metals* 2019, 521-531.
7. Amit Gupta and Biswajit Basu, Sustainable primary aluminium production – technology status and future opportunities, *Transactions of the Indian Institute of Metals*, Volume 72, Issue 8, 2019, 2135–2150.
8. Asbjørn Solheim, Some aspects of heat transfer between bath and sideledge in aluminium reduction cells, *Light Metals* 2011, 381-386.
9. Asbjørn Solheim et al., Sideledge in Aluminium Cells: Further Considerations Concerning the Trench at the Metal-Bath Boundary, *Light Metals* 2019, 787-793.
10. Asbjørn Solheim, Henrik Gudbrandsen and Sverre Rolseth, Sideledge in aluminium cells: the trench at the metal-bath boundary, *Light Metals* 2009, 411-416.
11. Asbjørn Solheim, Nils-Håvard Giskeødegård, and Nancy J. Holt, Sideledge facing metal in aluminium electrolysis cells: freezing and melting in the presence of a bath film, *Light Metals* 2016, 333-338.
12. Mark P. Taylor et al., The dynamics and performance of reduction cell electrolytes, *Light Metals* 1990, 259-266.
13. P-Y. Geay, Barry J. Welch, and Pierre Homsi, Sludge in operating aluminium smelting cells, *Light Metals* 2001, 541-547.
14. Daniel Whitfield et al., Metal pad temperatures in aluminium reduction cells, *Light Metals* 2004, 239-244.

15. Asbjørn Solheim et al., Liquidus Temperatures for Primary Crystallization of Cryolite in Molten Salt Systems of Interest for the Aluminium Electrolysis, *Metallurgical and Materials Transactions B*, 27, 1996, 739-744.
16. Egil Skybakmoen, Asbjørn Solheim, and Åsmund Sterten, Alumina Solubility in Molten Salt Systems of Interest for Aluminium Electrolysis and Related Phase Diagram Data, *Metallurgical and Materials Transactions B*, 28, 1997, 81-86.
17. Tabsh, M. Dupuis and A. Gomes, Process Simulation of Aluminum Reduction Cells, *Light Metals* 1996, 451-457.